# Changes in the fire resilience of Mediterranean trees in response to climate variability over the past 300 Years

Bulle I. Alberto (1,2,3) \*, Justin Badeau (1,2,4), Frédéric Guibal (4), Aurèle Baretje (2,5), Jean-Christophe Domec (3,6), Christopher Carcaillet (1,2) \*

- (1) École Pratique des Hautes Études, Paris Sciences Lettres University (EPHE-PSL), Paris, France
- (2) Université Claude Bernard Lyon 1, LEHNA UMR5023, CNRS, ENTPE, Villeurbanne, France
- (3) Department of forestry, Bordeaux Sciences Agro-INRAE UMR ISPA, Gradignan, France
- (4) Mediterranean Institute of marine and terrestrial Biodiversity and Ecology, IMBE, CNRS (UMR 7263), Aix Marseille Université, France
- (5) École Normale Supérieure de Lyon, Lyon, France
- (6) Nicholas School of the Environment, Duke University, Durham, North Carolina, USA \*Authors for correspondence: <a href="mailto:bulle.alberto@etu.ephe.psl.eu">bulle.alberto@etu.ephe.psl.eu</a>, <a href="mailto:christopher.carcaillet@ephe.psl.eu">christopher.carcaillet@ephe.psl.eu</a>

Key words: Fire, Radial growth, Tree-ring, Drought, Mediterranean, Forest, *Pinus nigra*.

# **Abstract**

With global warming, understanding the tree resilience to fire is still a scalding topic in ecology. Tree resilience would depend on fire intervals, and on interactions with atmospheric conditions, including temperature, precipitation, drought, and CO<sub>2</sub>. These interactions would be exacerbated in Mediterranean ecosystems. We test this hypothesis by analysing variations in tree-ring widths following fires, using growth

outside fire periods as reference. The study focused on black pine in Corsica as a model species to investigate long-term ecological responses to fire, based on fires spanning the past 300 years. Tree resistance and resilience to fire have progressively declined over the past three centuries, regardless of fire intervals and  $CO_2$ . Since the mid-19th century, recovery times have lengthened while resistance has weakened, correlating with precipitation and drought intensity. These results indicate that the combined effects of drought intensity and fires endanger tree survival by compounding their impacts on post-fire recovery.

#### INTRODUCTION

Climate change is altering forest disturbance regimes, including wildfires (Seidl et al., 2017). Disturbances involve the partial destruction of biomass (Grime, 1977) and are spatially and temporally discrete (Pickett & White, 1985). They can disrupt ecosystem functioning and alter long-term ecosystem resilience, i.e. the capacity of an ecological system to recover rapidly its structure and function after disturbance (Holling 1973; Lockwood and Pimm, 1995) questioning their adaptation facing the climate change.

At the global scale, fire frequencies are either decreasing or remaining stable, depending on regions (Andela et al., 2017; Cunningham et al., 2024), while the vulnerability of human populations to fire is increasing (Seydi et al., 2025). In the Mediterranean biome, the extent of extreme wildfires is increasing (Cunningham et al., 2024), as they spread into new areas that were previously protected by elevation or precipitation (Fréjaville & Curt, 2014). Climate-based models predict an increase in the likelihood and frequency of burnt areas (Turco et al., 2018; Ruffault et al., 2020).

Mediterranean ecosystems are generally fire prone due to dry and hot summers, as evidenced by the presence of fire-adapted species bearing specific life traits of varying flammability levels (Keeley et al., 2011; Pellegrini et al., 2023). Over past centuries, some southern European ecosystems, e.g., those dominated by black pine (*Pinus nigra* Arnold), experienced non-lethal repeated fires (Christopoulou et al., 2013; Fulé et al., 2025). Their frequencies changed over time, with mean fire intervals ranging from 5 to 60 years (Sahan et al., 2022; Badeau et al., 2025). This reveals a degree of resilience, as supported by the high number of fire scars, sometimes more than ten per tree (Christopoulou et al., 2013; Sahan et al., 2022; Badeau et al., 2024).

The survival of trees subjected to repeated fires has long been documented (e.g., Zackrisson, 1977; Swetnam, 1993), but this remains largely unexplored for Mediterranean species. Addressing this gap is critical for anticipating fire-driven ecosystem shifts. The present study aims to assess the pattern and duration of post-fire growth, as expressed through tree-rings width. The duration and pattern of post-fire recovery of tree growth remain poorly understood, raising questions about the underlying mechanisms of resistance (Connell & Sousa 1983) and resilience or recovery time (Holling, 1973, Schwarz et al., 2020), which partly depends on resistance itself (Hodgson et al., 2015; Carcaillet et al., 2020).

In black pine forests, past fire intervals may have been shorter than 30 years for several centuries (e.g., Leys et al., 2014; Sahan et al., 2022). Given that trees have survived such repeated fires, it can be assumed that pines are intrinsically resilient to short mean fire intervals (hereafter, MFI), maintaining stable growth rates. However, we hypothesised that longer fire intervals may enhance growth by allowing more complete recovery. Nonetheless, the relationship between MFI and tree growth may have shifted over the past three centuries due to change in atmospheric conditions. These include elevated atmospheric CO<sub>2</sub> concentrations (Rubino et al., 2019), rising temperatures (Luterbacher et al., 2004), altered precipitation regimes (Pauling et al., 2006), and more frequent droughts in recent decades (Cook et al., 2015). Depending on their interactions, such environmental changes may have either enhanced or constrained tree physiology: rising CO<sub>2</sub> levels could potentially stimulate tree growth through increased photosynthesis, particularly when nutrient availability also increases (Ainsworth & Long, 2004).

Conversely, warmer and drier conditions are expected to reduce growth by increasing thermic and hydric stress and reducing resilience. In some cases, elevated  $\mathrm{CO}_2$  may also exacerbate stress by increasing photosynthetic demand beyond resource availability. Independently of the fire interval, we also hypothesised that pine resistance and resilience to fire should progressively decrease over time due to climate warming.

By integrating tree-ring measurements on black pine with fire history and long-term climatic trends, our study provides a rare insight into how trees respond to repeated fires across centuries. It sheds light on the resilience of Mediterranean forests under compounding disturbance and climate pressures, with implications for anticipating ecosystem tipping points in fire-prone biomes.

# **MATERIALS AND METHODS**

# Study area

The Study area is situated in Corsica, a northwestern Mediterranean island (Figure S1a). The Corsican climate is hot and dry in summers, and cool and wetter in winters, but the island's orography leads to cold seasonal conditions, with up to five months of intermittent snow cover in winter. On average, Corsican annual temperature is 13.6°C and annual precipitation 803 mm. The study ecosystem is the montane forest dominated by black pine. Trees were sampled at four sites distributed along a north-south transect on the east-facing slope of the Corsican cordillera (Figure S1), at elevations averaging between 1100 and 1440 m (Table S1). All canopies were dominated by black pines, although a few maritime pines (*Pinus pinaster* Aiton) occurred below 1100 m. The plots were homogeneous in terms of topography and vegetation, both between and within sites.

# Tree sampling and sample preparation

A total of 270 individuals - including living trees, snags, logs, and stumps - were collected using chainsaws in 5 to 6 plots per site, selected for the highest number of visible scars (Farris et al., 2013). On average, 12 trees were sampled per plot, with values ranging from 5 to 21 (Table S2). Samples were air-dried and sanded with progressively finer grits up to P400, to obtain smooth surfaces with cells visible under a microscope (×100). Samples were then digitized using a scanner at 1200 dpi. Ring-widths were measured from scanned images in Coorecorder software and the quality control of crossdating was carried out with Cofecha software (Holmes, 1983). The measure was made as far as the scar as possible to avoid any deformations (Micco et al., 2013, Figure S2). In total, 180 trees (67%) were successfully crossdated with the reference chronology FRAN027 (AD 1518-1980; ncei.noaa.gov/access/paleo-search/study/4389). This chronology was completed by our own reference series based on 34 living, unscarred trees sampled in burnt plots using increment borers (hereafter control trees), resulting in a mean of 8 crossdated fire-scarred samples per plot (Table S2).

# Fire history

The fire reconstruction, including fire years, mean fire intervals (MFI), and the classification of four distinct MFI periods (two with short and two with long intervals), was based on the dendrochronological dataset and methods detailed in Badeau et al., (2025, Table S3). In summary, the 180 crossdated trees revealed 567 fire scars, each assigned to

a specific year. The oldest fire was dated to 1635 at Tartagine. However, only fire scars reported on at least two trees per site were used, yielding a final fire chronology of 487 scars on 174 different trees. The very first interval of 60 years at Tartagine, between 1659 and 1719 was excluded as outlier and abnormal for the 17<sup>th</sup> century (Figure S1b). For the present purpose, the period covering enough fire years to reconstruct MFI started with the 1719 fire in Tartagine until the last in 2012 in Vivario. The MFI chronologies for each site ended in 2024, including the last incomplete interval corresponding to the time since the last fire. Overall, 51 fire intervals were obtained, but including these incomplete fire-free intervals, a total of 55 intervals was considered (Badeau et al., 2025). It produced a synthetic chronology of fire intervals (Figure S1b, Table S3).

MFI ranged from  $12 \pm 7$  years at Melo to  $22 \pm 19$  years at Tartagine, with no significant differences between sites in terms of MFI (Table S4) nor in terms of low stochasticity (cf. coefficient of variation all < 1.0). Four distinct periods were identified (Fig S1c; Table S4), two with short intervals (1719-1848 (P1) and 1923-1970 (P3)) and two with long intervals (1849-1922 (P2) and 1971-2024 (P4)). The periods of short MFI were not different from each other, as were the long MFI periods from each other, but short and long periods differed significantly from each other (p < 0.001, Figure S1c).

# Atmospheric data

Seasonal precipitation (Pauling et al., 2006; AD 1500-2000) and temperature reconstruction data (Luterbacher et al., 2004; AD 1500-2002) were downloaded from ClimateExplorer (https://climexp.knmi.nl/). These data were gridded for the area situated between 41° and 44°N and between 5° and 13°E, which captures Corsica, western Italy and southeastern France, and enough weather stations to align and stabilise the climatic reconstructions. As these reconstructions extended only until 2002, additional data from METEO-France (the French meteorological agency, https://meteo.data.gouv.fr) were incorporated to extend the series to 2022. To achieve this, both series were standardized over a common reference period [1970-1990] which minimized the differences between them, expressing them as z-scores. The Palmer drought severity index (PDSI, AD 1-2012) was inferred from reconstruction of the Old World Drought Atlas, OWDA (Cook et al., 2015) and the global CO<sub>2</sub> data over the past centuries resulted from ice core records (Rubino et al., 2019).

# Data analysis

All numerical analyses were carried out under the R statistical environment version 4.4 (R Core Team, 2024).

All annual ring-widths were detrended using a cubic smoothing spline with a 65-year frequency response to remove the low-frequency trends, producing tree-ring indices (TRI). To assess tree responses to fire through TRI inter-annual variability, we applied Superposed Epoch Analysis (SEA; Swetnam, 1993) using the standard method implemented in *burnR* package (Malevich et al., 2018). The SEA evaluated changes in the mean TRI by comparing TRI values before and after fires to those from a selected period including those fires. To do so, the standard SEA method (Malevich et al., 2018) establishes by bootstrapping a null distribution based on actual data but without fire effect, allowing us to compare the mean tree-ring width during observed fire years to ring-width expected by chance. Confidence intervals (CI) are derived from 1000 Monte Carlo simulations.

SEA analyses were conducted both on the complete dataset (all fires pooled) and separately for each mean fire interval (MFI) period. Between 1719 and 2012, we identified 487 fire sequences corresponding to 54 distinct fire years. Each sequence covered 16 years: 5 years before, the fire year, and 10 years after.

The bootstrap procedure of SEA was not adapted to account for variable sample sizes across years, which were incompatible with the original *burnR* script. Therefore, a first dataset of observed fire TRI values was constructed, with rows corresponding to fire years and columns corresponding to 16-year TRI sequences (–5 to +10 years around each fire). Then, 1000 random matrices of identical dimensions were generated by randomly reassigning individual–fire combinations for each fire year, reproducing the observed number of fire events. Each row in these matrices represented a "pseudo-fire year" associated with TRI sequences unrelated to actual fires. These randomized datasets were used to construct the null distribution for SEA comparisons against the observed fire dataset.

Tree vulnerability (h) was defined as the TRI difference between expected (null-model) growth and observed post-fire growth. Since the year+1 consistently showed the strongest reduction in TRI (Schwarz et al., 2020), its value was used to calculate h, and tree resistance ( $\omega$ ) was then calculated as  $\omega = 1-h$ .

A Principal Component Analysis (PCA) was carried out on the TRI to explore their response patterns beyond those identified by the SEA. Because PCA requires complete data, only 413 of the 487 identified fire scars (corresponding to 16-year fire sequences) were included in the PCA, followed by a cluster analysis. We clustered the responses to identify the main patterns of reactions in terms of TRI using the *kmeans* method (Hartigan & Wong, 1979) and the *cluster* function from the *stats* package. The cluster number was determined by a bootstrapping method using the *clusterboot* function from the *Flexible Procedures for Clustering* (*fpc*) package and from visualisation of the data using dimensional reduction. To assess the association between clusters and periods, a chi-squared test of independence was performed using the *chisq.test* function. Standardized residuals were calculated to identify where the observed frequency deviates significantly from the expected frequency under the independence assumption. Absolute values greater than 2 indicate a substantial contribution to the association.

To assess the influence of atmospheric variables (CO<sub>2</sub>, precipitation, temperature, and PDSI, using annual or seasonal values) as potential drivers of tree growth in terms of TRI, we calculated pairwise correlations among these variables, as well as between each variable and the mean TRI per period. Pairwise comparisons between periods were conducted using Wilcoxon rank-sum tests with Holm correction for multiple testing, implemented with the *stats* package.

To evaluate the relationship between atmospheric variables and annual radial growth, we computed Spearman correlations (*rs*) using the *cor* function from the R\_*stats* package. Given the presence of autocorrelation in the time series, we used block permutation tests to assess the significance of the correlations.

#### **RESULTS**

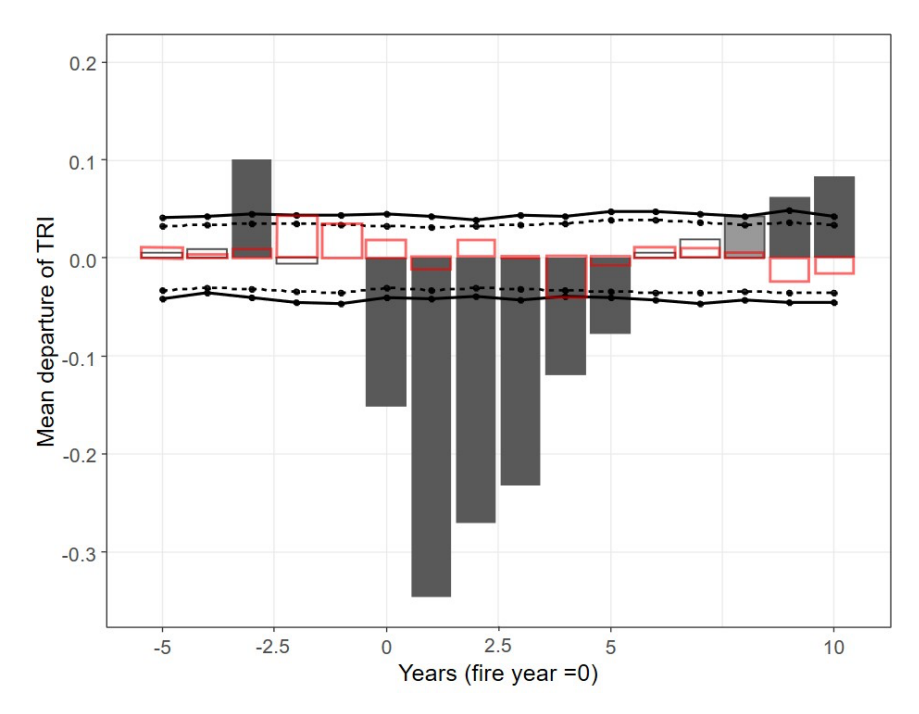


Figure 1. Pattern of radial tree growth. In shades of grey: response to fire based on superposed epoch analysis (SEA) carried out on 487 fire sequences, derived from all scarred trees across the four sites, corresponding to 54 fire events occurring between 1719 and 2012. The SEA showed the difference between the mean tree-ring index (TRI) over a 16-year period centred on the fire year (year+0) and the mean TRI calculated over 16-year periods in the chronology that did not include the fire events. Significant departures are shown in light grey (95%  $\leq$  Confidence Interval < 99%) or in dark grey (CI  $\geq$  99%). In red outline, the pattern of radial tree growth based on SEA, derived from 34 unscarred trees used as control trees and for the same fire years. CI are identical thus represented in bold.

# The whole sequence, from 1719 to 2024

The SEA highlighted the average response of TRI to fire events. Figure 1 shows the TRI response to all fire events between 1719 and 2012, whatever the MFI period. Growth rates were significantly reduced (99% CI) during and following the fire year. These reductions were the most severe in the first year (year+1) after the fire year (year+0) and lasted up to five years after the fire, totalling six years of significant reduction. A gradual recovery occurred, illustrating a resilience of six years on average, from year+0 to year+5. The general trend followed a sinusoidal pattern with low values after the fire year and values higher than the trend from year+8 (95% CI) to +10 (99% CI; Figure 1). In contrast, the control group showed no significant effect and no trend comparable to that of the scarred trees (insert Figure 1).

The cluster analysis of TRI sequences yielded four distinct and evenly distributed clusters (Figure 2a, Table S5). The first cluster represented complacent TRI sequences, showing no significant change in ring-width following the fire year compared to preceding years. The second cluster comprised sequences with initially reduced ring-widths that declined further post-fire before gradually recovering over 7 years. The third cluster group included trees with large pre-fire TRI that experienced sharp post-fire decreases, requiring approximately 10 years for full recovery. Finally, the fourth cluster exhibited fire-enhanced

growth: trees with lower pre-fire ring-widths showed significant TRI increases persisting for at least 7 years post-fire. This cluster analysis highlights that not all trees reacted uniformly.

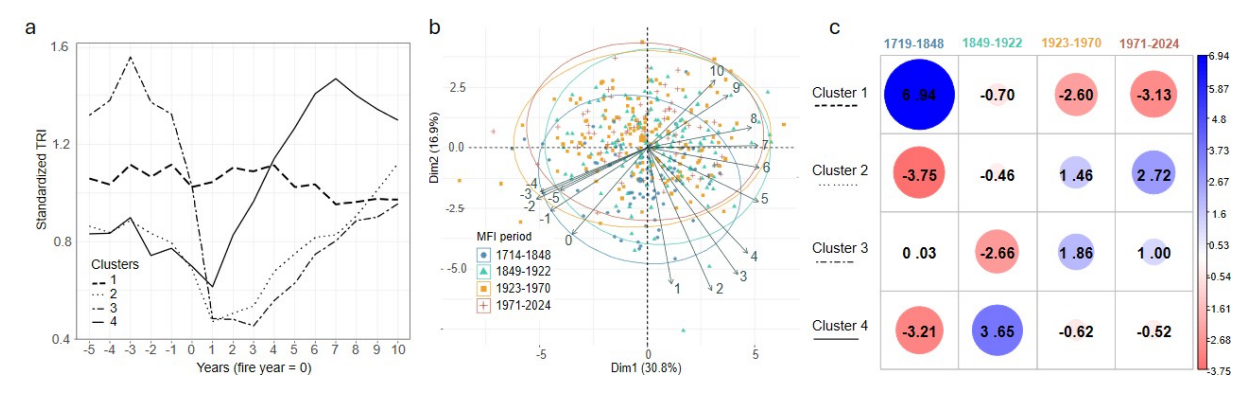


**Figure 2.** (a) Mean patterns of response of tree-ring index (TRI) per clusters from the k-means algorithm based on the 16-year sequences coordinates on the Principal Component Analysis (PCA) showing one complacent cluster (1) and three sensitive clusters (2-4). (b) PCA biplot of the response of radial growth of all scarred trees grouped per mean fire interval (MFI) period between 1719 and 2012. The first two principal components explained 47% of the total variance. Each symbol represents one of the 413 complete fire sequences of 16 years of TRI associated with a fire year and is coded per MFI period. The arrows represent the active variables used in the PCA and the numbers correspond to years of the fire sequence, e.g., 0 is the fire year, -2 is two years before, 4 is four years after. (c) Standardized residuals from the chi-squared test, indicating the observed frequency contribution of a cluster in a period relatively to the expected frequency under the independence assumption.

The PCA revealed a clear contrast among time points (years *versus* fire year): pre-fire years cluster in the bottom left of the biplot, post-fire years (+9 and +10) appearing on the opposite side (upper right), and the year immediately following the fire being orthogonal to this diagonal (Figure 2b). PC1 captured a temporal gradient ranging from the five years preceding the fire year, including the fire year (negative side), toward years after the fire (positive side) during which TRI values initially decreased (year+5) due to fire effects and then recovered (+6 to +8; Figure 2b). PC2 contrasted the immediate post-fire years on the negative side, i.e. years +1 to +4, with the later recovery phase, +9 and +10 (Figure 2b), which showed values higher than on average before the fire (Figure 1). PC2 expresses TRI range from the minimal values on the negative side, to the maximal values on the positive. No strong pattern was apparent in the distribution of individual points ('trees') based on TRI (Figure 2b). The ellipse corresponding to the 1719-1848 fire period (P1) was mainly stretched by the negative side of PC2, whereas the other ellipses mainly overlapped (Figure 2b). Moreover, the ellipse for P1 was less extensive than those of the other three periods, indicating lower variability in values.

The complacent tree-rings (cluster 1) were significantly overrepresented in tree-rings in P1 (standardized residual = 6.34) and underrepresented in later periods (Figure 2c). Cluster 2 contrasted periods, being less common P1 and more prevalent in recent periods notably in 1971-2024 (P4) (residuals > 2). Cluster 3 was consistently represented across all MFI periods (residuals < 2). Finally, the cluster 4 was particularly widespread during the 1849-1922 period (P2) (residual = 3.65). Periods characterized by short MFI (1719-1848)

and 1923-1970) did not exhibit similar TRI patterns illustrated by clusters, nor even for periods with long MFI (1849-1922 and 1971-2024; Figure 2c).

# Analyses per period of mean fire interval

SEA analyses were carried out separately for each of the four MFI periods to assess tree radial growth responses relative to pre-fire growth rates and to evaluate the consistency of response patterns across different fire regimes (Figure 3a). Even though each period displayed response patterns rather distinct from the overall trend (Figure 2), general patterns indicated a decline in both resistance and resilience of tree growth following fires over the past three centuries.

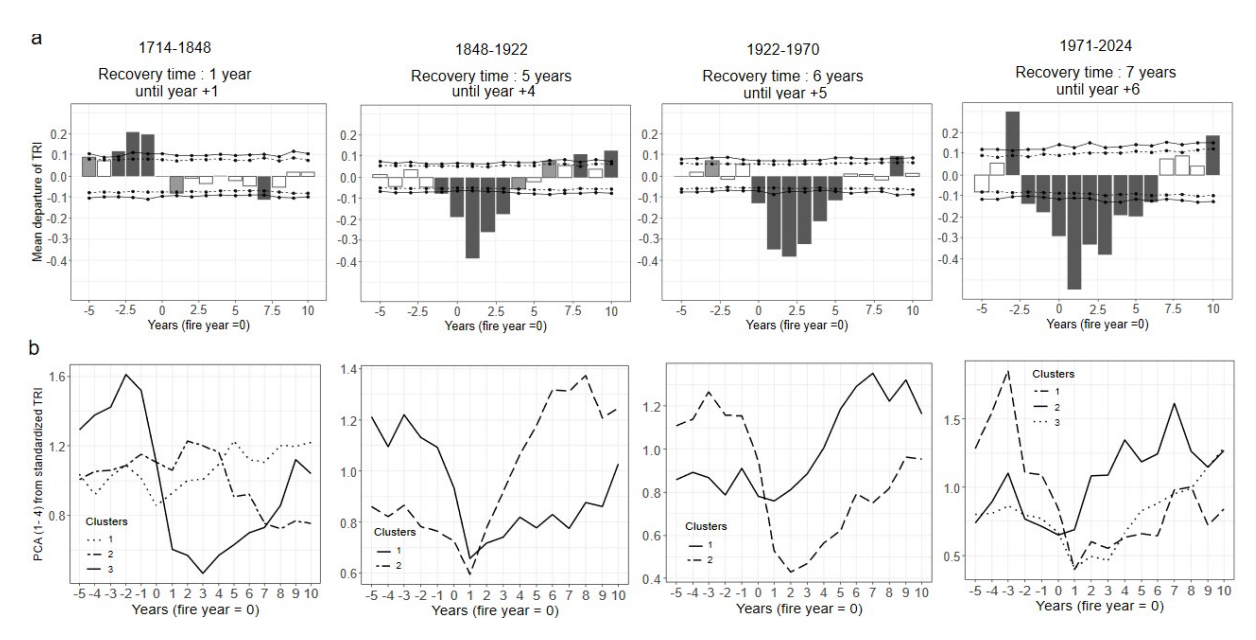


**Figure 3.** Tree-ring responses per period of mean fire interval (MFI); (a)\_Superposed epoch analyses (SEA); the figure illustrates the difference between the mean tree-ring index (TRI) calculated over 16-year sequences centred on fire years (year+0), and the mean TRI derived from 16-year sequences in the chronology that exclude the fire year. Significant departures are shown in light grey (95%  $\leq$  CI < 99%) or in dark grey (CI  $\geq$  99%). (b) Cluster-based analyses from the k-means algorithm of TRI responses by MFI period.

Regarding P1, only the year+1 exhibited a significant decrease (95% CI), while the treering index (TRI) declined from year0 to +10 but without being significant (Figure 3a). Cluster-based analysis revealed three main responses associated to P1 (Figure 3b). Clusters 1 and 2 were unaffected by fire (complacent sequences), though cluster 2 showed a delayed TRI decrease starting six years after fire. In contrast, cluster 3 showed elevated pre-fire TRI, followed by a sharp post-fire decline and recovery by year+8.

From P2 onward, the general pattern observed in figure 2 began to emerge. TRI decreased significantly (99% CI) from year-1, remained low until year+4, and recovered by year+5. Two contrasting clusters emerged: one showing strong decline and decade-long recovery; the other displaying enhanced growth from year+2 onwards.

P3 followed a similar trajectory, but pre-fire levels were only reached by year+6. Two clusters were evident: one marked by a sharp post-fire decline and gradual recovery by

year+8, and another in which trees showed a lasting increase in TRI from year+3 to +6 before stabilizing.

During P4, ring-width started declining from year-2, with low values persisting until year+6. Three response clusters were identified: two clusters showed post-fire declines followed by slow recovery, while the third one consisted of trees with enhanced growth in the years following the event (year+1).

The proportions of sequences in each cluster for each period are mainly evenly distributed, except a prevalence (79%) of the complacent series in P1 (clusters 1 et 2 in Figure 3, Table S5).

Across the four periods (Figure 3), a clear temporal trend emerged: (i) year+1 was always the most impacted year, (ii) TRI values at year0 and +1 decreased progressively from one period to the next, and (iii) the duration of post-fire recovery stretched from one year in the 1719-1848 period to seven years in 1971-2024.

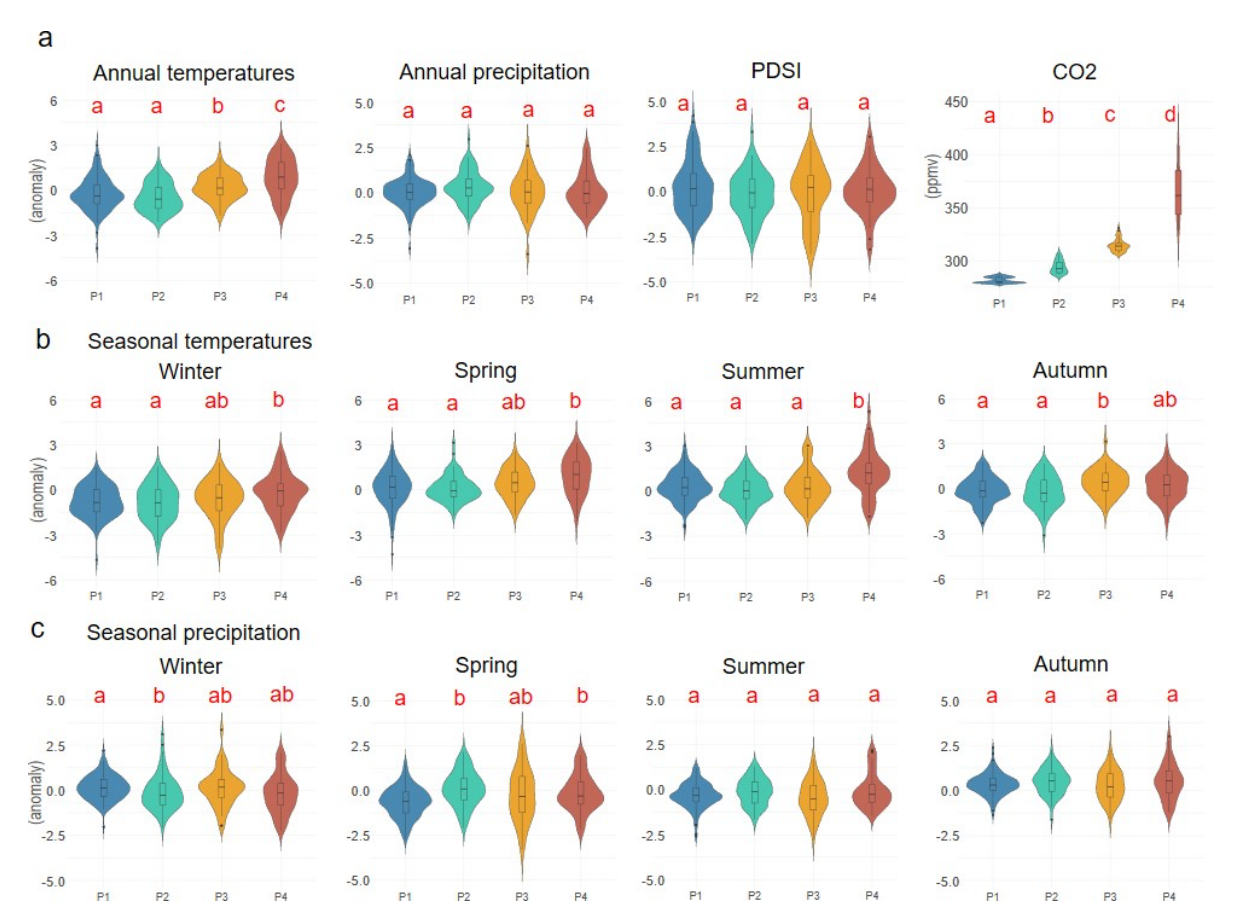


**Figure 4.** Distributions of mean climatic and atmospheric values across the mean fire intervals (MFI) periods. (a) Annual temperature, annual precipitation, Palmer Drought Severity Index (PDSI), and atmospheric  $CO_2$  concentration, (b) seasonal temperature, and (c) seasonal precipitation. Violin plots show the distribution of standardized values expressed in anomalies, except for  $CO_2$ , expressed in ppm. Red letters indicate post-hoc results from the Wilcoxon test (different letters = significant differences at p < 0.05).

# Climate trends associated to MFI periods

Climatic conditions were analysed per MFI period (Figure 4). They differed among the four MFI periods in terms of trends of temperature, precipitation, PDSI, and atmospheric CO<sub>2</sub> concentration. Temperatures were relatively stable between the first period (P1, 1719-1848) and the second (P2, 1849-1922), then rose from the mid-19th century onward. P3 (1923-1970) was significantly warmer than P1 and warming intensified during P4 (1971-2024) in winter, spring and summer, which was the hottest period across all seasons (Figure 4, Figure S3). Annual, summer and autumn precipitation showed no significant variation, but P1 was drier than P2 and P4 in spring and wetter in winter than P2. PDSI remained stable among periods, indicating no major shift in drought conditions despite increase in spring and summer temperature. In contrast, atmospheric CO<sub>2</sub> increased continuously, with all pairwise differences being significant (Figure 4, Figure S3).

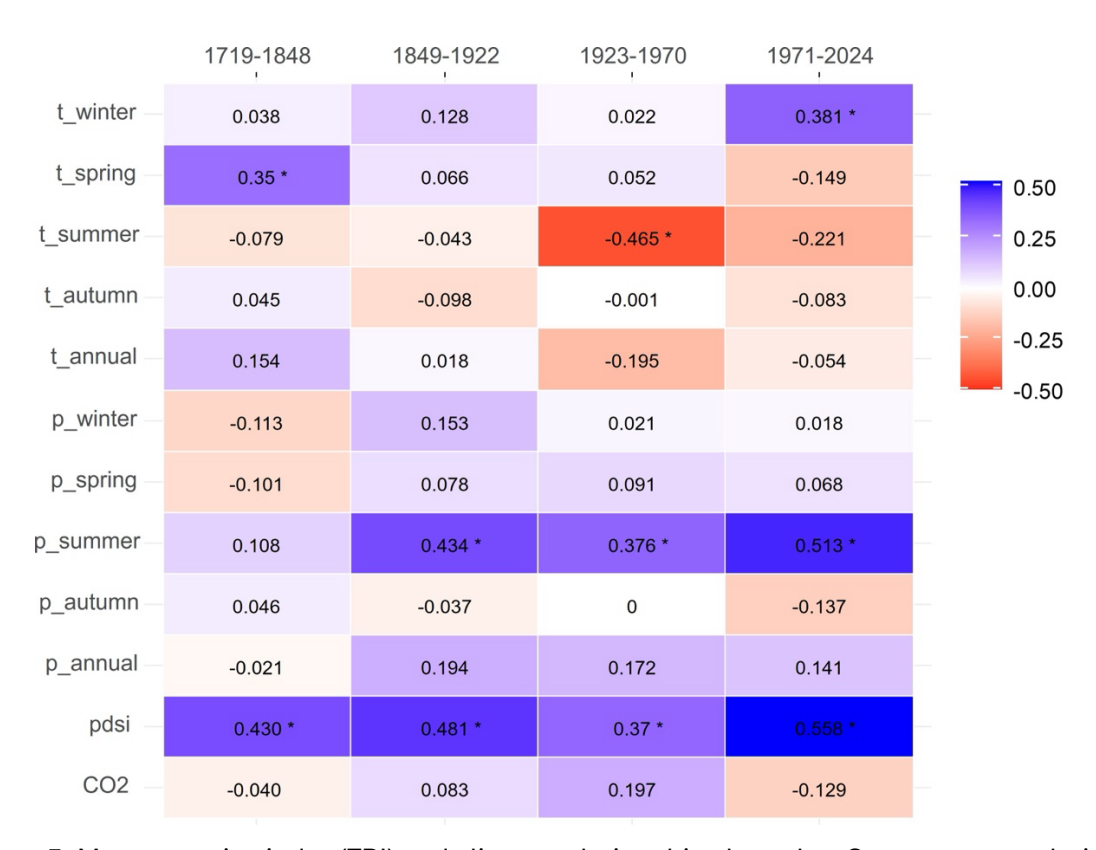


**Figure 5.** Mean tree-ring index (TRI) and climate relationships based on Spearman correlation (*rs*) analysis ('Corrplot') of mean annual ring width and atmospheric variables for each of the four periods of mean fire interval (MFI). Red indicated a negative association and blue a positive one; the colour intensity illustrates the level of the relationships. The letters "t" and "p" associated with each season represent temperature and precipitation, respectively.

# Climate-TRI relationships per MFI period

Overall, TRI was positively correlated with PDSI and summer precipitation across all periods, and negatively with summer temperature (Figure 5). In detail, TRI issued from different MFI periods can be positively correlated with winter temperature (P4) or spring temperatures (P1), which is in depth analysed hereafters for all atmospheric variables.

Mean TRI values per period were significantly positively correlated with PDSI (0.369 < rs < 0.559) and summer precipitation (0.375 < rs < 0.514); Figure 5). The correlation with the PDSI was weaker during P3, which also exhibited the highest interannual variability in precipitation. Similarly, the correlation with summer precipitation was reduced during P1 (Figure 5), when temperatures were lower in all seasons and spring precipitation as well (Figure 4). Correlations with precipitation in other seasons were generally low and not significant. Overall, precipitation appeared to limit growth during P1, while slightly positive correlations were observed in the three subsequent MFI periods, except for autumn precipitation.

The influence of temperature on TRI varied across MFI periods. Summer temperatures were negatively correlated with TRI in all periods, whereas winter temperatures tended to promote TRI. Specifically, TRI during P1 were positively correlated with spring temperature (rs = 0.350), TRI during P3 were strongly negatively correlated with summer temperature (rs = 0.465), and, during P4, TRI were positively correlated with winter temperature (rs = 0.381; Figure 5).

Although atmospheric  $CO_2$  steadily increased over the past 300 years, TRI variations were not significantly correlated with this variable. The highest, though still non-significant, correlation was observed during P3 (rs = 0.197), coinciding with the period when TRI showed its strongest association with summer temperatures.

After P1, when fire resistance decreased and recovery times increased, TRI showed stronger negative correlations with temperature, while correlations with precipitation, which had previously limited growth, became positive. The exceptions were for winter temperatures and autumn precipitation, which became positive and negative, respectively (Figure 5).

#### **DISCUSSION**

Consistent with our main hypothesis, our results demonstrated that black pine resistance and resilience to fire progressively decreased over the past three centuries (Figure 1), although not all trees behaved similarly (Figure 2). Each period showed a somewhat distinct pattern in tree-ring growth responses (Figure 3), which was not related to the MFI but to climatic features and notably to PDSI (Figure 5). Hereafter, we discuss the ecological drivers underlying these changes and their implications for forest resilience under future fire regimes.

# Resistance and resilience to fire

Our analyses reveal a consistent pattern of black pine response to fire events over the past 300 years. Tree-ring width decreased most markedly during the first year following the fire. This was expected, as most fires occur in summer since the 17<sup>th</sup> century in Corsica (Badeau et al., 2025), in similar proportion than in other Mediterranean forests since the 16<sup>th</sup> century (Sahan et al., 2022). Trees typically recovered their growth pattern within six years. Interestingly, between the 8th and 10th years after fire, the SEA of TRI displayed higher values, producing a sinusoidal pattern over the 16-year sequence (Figure 1). Due to the rarity of intervals exceeding ten years between fires in our dataset, particularly during the short MFI periods (1719-1848 and 1923-1970), it was not possible to analyse the post-fire tree responses beyond ten years. Nevertheless, our results

clearly show that the first post-fire year was the most critical and constituted a proxy for tree resistance, while the full recovery time reflected resilience. Combining these two components, the resilience of black pine has deteriorated over the past 300 years (Figure 6).

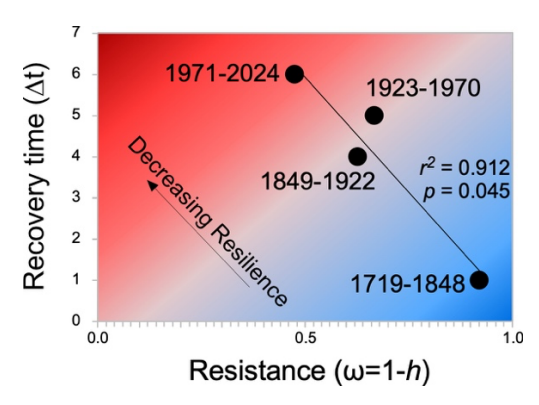


**Figure 6.** Relationship between resistance (h) and recovery time ( $\Delta t$ ) across MFI periods. Each point represents a mean value for the corresponding period; a significant positive correlation is observed ( $r^2 = 0.912$ , p = 0.045).

Compared with other studies on tree-ring response to fire, ours is exceptional in terms of number of fire events (54), chronology duration (300 years), and sample size (180 crossdated scarred trees plus 34 controls). Previous investigations typically analysed far fewer events, e.g., 2 to 5 events in Aleppo pine (*P. halepensis* Mill.) or maritime pine, or over shorter post-fire periods (Battipaglia et al., 2014; Niccoli et al., 2019), thus limiting their capacity to detect long-term modifications in tree response to disturbance.

For black pine, only two studies applied SEA to tree-ring indices, measuring post-drought responses up to 5 years (Martin-Benito et al., 2018) or 3 years (Lévesque et al., 2014). These post-disturbance chronologies were shorter than ours and focused on a limited number of 20th-century events, restricting their ability to detect long-term modifications in tree responses to disturbance under global climatic changes.

In natural settings, Martin-Benito et al. (2018) showed that dominant black pine trees in southern Spain recovered faster but more variably within two years compared to suppressed trees, likely due to differences in moisture and light availability. In black pine plantations, Lévesque et al., (2014) found that resilience was achieved within one year after drought, with site-specific variations depending on soil and local climate conditions. This last study matched our outcomes showing that tree response to non-climatic disturbances is partly modulated by climatic features.

The observed increase in TRI width between years+8 and +10 may reflect compensatory growth mechanisms, such as improved water uptake and transpiration by foliage that gradually recovered after being damaged by fire (Bär et al., 2019), enhanced nutrient availability from ash deposition (Roshan & Biswas 2023), or increased soil nitrification due to charcoal accumulation (DeLuca & Sala 2006), or more simply less competition by lowering stand density (Zhang et al., 2019).

# Temporal variability in tree responses to fire

The general and average pattern varies between trees and over time (Figure 2, Figure 3). Over the past 300 years, four main behavioural patterns could be highlighted, including trees that did not respond to fire in terms of radial growth (cluster one in Figure 2), despite

fire scars evidencing that these trees were affected by losing some of their cambium and vascular tissues. Some trees grew better before the fire than after (cluster 3 in Figure 2) and did not recover within 10 years, revealing a net and lasting impact of fire. The survival of these trees may be jeopardized if the MFI remains under 10 years for extended periods. Others showed a net impact with two types of responses. Some of these impacted trees showed resilience within approximately five years (cluster 2) in accordance with the general and average trend (Figure 1), while others showed a cumulative growth increase two or more years after the fire compared to the pre-fire reference period.

This inter-tree variability can have different origins, such as the spatial variability of fire intensities including within a fire (the fire intensity is never uniform on a scale of a few meters) that has aftermaths on nutrients through organic matter consumption, tree age, genetic variability, tree-density around scarred trees (competition for water and nutrients), soil (depth) and topography slope. Trees behaving differently to fire has not changed through periods (Figure 3) indicating that the four clusters highlighted did not result from different behaviour due to MFI variation. Thus, this result does not support our working hypothesis which proposed that fire intervals over decades could control for the resilience of black pine. Fire per se, and their frequencies are not the Achilles' heel of the resilience alteration to fire event. Because the decreasing trend of resistance and resilience is progressive over the past 300 years (Figure 6), the main driver is probably atmospheric.

#### PDSI and summer conditions control resistance and resilience of black pine

Climate appears to be the primary driver of the long-term changes in resistance and resilience; climatic characteristics have modified resistance and recovery time since the 18<sup>th</sup> century. Interestingly, although annual and seasonal temperature and CO<sub>2</sub> have been the main atmospheric changes over the past 300 years (Figure 4), trees have mainly interacted with drought and summer precipitation (Figure 5) despite the low variability of these features. Higher PDSI values and greater summer precipitation were associated with enhanced post-fire radial growth. The PDSI formula uses precipitation and temperature values to determine plant dryness, through moisture supply and demand using a water balance model (Van Loon 2015). Since 1970, the response of TRI to PDSI values have been driven by rising temperatures, which, in Corsica, have progressively offset the slight influence of precipitation changes over the past 300 years (Figure 4). This resulted in an increased dependence of trees on summer precipitation.

Such effect of precipitation and more generally PDSI on tree-ring could have been predicted based on the studies in natural conditions (Martin-Benito et al., 2018) or plantations (Lebourgeois 2000; Lévesque et al., 2014) who evidenced that black pines were sensitive to drought, mostly during the growth of late-wood (Martin-Benito et al., 2018), *i.e.* in summer and autumn (Häusser et al., 2021; Sahan et al., 2024). This interaction between fire and drought reveals a cascading effect of climate on the disturbance (Buma 2015): without climatic effect, fire display low-to-moderate severity, whereas with drought the fire severity is increased according to degraded resistance and recovery time. This question concerns the future of the black pine in Corsica, knowing that climate change is expected to increase the frequency and duration of heat waves and droughts (Turco et al., 2018; Ruffault et al., 2020). If fire frequency remains moderate (long MFI) as has been the case since the 1970s (Badeau et al., 2025), largely due to fire suppression policies (Fréjaville et al., 2018), the effect of climate on tree dynamics is

expected to be moderate. However, as shown by our data and studies (Cunningham et al., 2024), the extreme fires and the complex effect of drought and fire risks could lastingly jeopardize black pine in its natural range in the Mediterranean basin.

Figure 3 highlights a slight but significant decrease in TRI one year before the fire year during the two periods of long MFI, P2 and P4. It cannot be excluded that climatic stress already affected trees in the year preceding the fire. This phenomenon possibly requires a specific and in-depth analysis of the relationship between climate variability and fire occurrence, as well as its potential consequences for tree response to fire.

#### CONCLUSION

Our tree-ring analyses shows a progressive and long-term decline in the fire resistance and resilience of black pine over the past three centuries, largely driven by increasing drought rather than mean fire interval, temperature, or  $CO_2$ . The findings highlight the growing vulnerability of Mediterranean forests to disturbances under a drying climate. Future research should quantify species-specific thresholds of drought tolerance, integrate physiological data to model recovery processes, and assess whether adaptive land management or even assisted seedling regeneration could enhance forest resilience under projected climate scenarios.

#### **AUTHOR CONTRIBUTIONS**

BIA, CC, and JCD conceptualized the study. AB, CC, FG and JB realized the field work. JB carried out the measurements. BIA realized the analyses. BIA, CC, JCD wrote the original draft. CC administrated the CorsicanFire and MedFire project. All authors were involved in the interpretation of the results and the final preparation of the manuscript.

#### **ACKNOWLEDGEMENTS**

Authors are indebted to Fabrice Torre (DREAL-Corse), Amandine Burguet-Mortti and Pasquale Moneglia (ENDEMYS), Olivier Riffard (Corsica administration), Peter Fulé (Northern Arizona University, Flagstaf) and also Sandra Guy, Antonella Massaiu and Germain Paolacci (ONF). Serena Felix (NAU, Flagstaff) assisted JB with analyses of samples.

# **CONFLICTS OF INTEREST**

The authors declare no conflicts of interest.

# **FUNDING INFORMATIONS**

Corsican DREAL (grant 2020-008) and the CIFRE Program (grant 2021-0058) both for funding the CorsicanFire project; the CNRS (grant: IEA00797) for the MedFire project; EPHE-PSL for a PhD grant to BIA.

#### **ORCID**

Carcaillet, Christopher 0000-0002-6632-150

Domec, Jean-Christophe 0000-0003-0478-2559

#### **REFERENCE**

- Ainsworth, E.A. & Long, S.P. (2005) What have we learned from 15 years of free-air CO2 enrichment (FACE)? A meta-analytic review of the responses of photosynthesis, canopy properties and plant production to rising CO2. *New Phytol.*, 165, 351–372.
- Andela, N., Morton, D.C., Giglio, L., Chen, Y., van der Werf, G.R., Kasibhatla, P.S., et al., (2017) A human-driven decline in global burned area. *Science*, 356, 1356–1362.
- Badeau, J., Fulé, P.Z., Guibal, F., Félix, S., Burguet-Moretti, A., Moneglia, P., & Carcaillet, C. (2025) Historical range of wildfire regime in black pine forests outside actual target of public policies. *J. Environ. Manag.*, 394, 127671. Doi: https://doi.org/10.1016/j.jenvman.2025.127671
- Badeau, J., Guibal, F., Fulé, P.Z., Chauchard, S., Moneglia, P. & Carcaillet, C. (2024) 202 years of changes in Mediterranean fire regime in *Pinus nigra* forest, Corsica. *For. Ecol. Manag.*, 554, 121658.
- Bär, A., Michaletz, S.T. & Mayr, S. (2019) Fire effects on tree physiology. *New Phytol.* 223, 1728-1741. Doi: doi/10.1111/nph.15871
- Battipaglia, G., De Micco, V., Fournier, T., Aronne, G. & Carcaillet, C. (2014) Isotopic and anatomical signals for interpreting fire-related responses in *Pinus halepensis*. *Trees*, 28, 1095–1104.
- Buma, B. (2015) Disturbance interactions: characterization, prediction, and the potential for cascading effects. *Ecosphere*, 6, art70.
- Carcaillet, C., Desponts, M., Robin, V. & Bergeron, Y. (2020) Long-Term Steady-State Dry Boreal Forest in the Face of Disturbance. *Ecosystems*, 23, 1075–1092.
- Christopoulou, A., Fulé, P.Z., Andriopoulos, P., Sarris, D. & Arianoutsou, M. (2013) Dendrochronology-based fire history of *Pinus nigra* forests in Mount Taygetos, Southern Greece. *For. Ecol. Manag.*, 293, 132–139.
- Connell, J.H. & Sousa, W.P. (1983) On the Evidence Needed to Judge Ecological Stability or Persistence. *Am. Nat.*, 121, 789–824.
- Cook, E.R., Seager, R., Kushnir, Y., Briffa, K.R., Büntgen, U., Frank, D., et al., (2015) Old World megadroughts and pluvials during the Common Era. *Science Adv.*, 1, e1500561.
- Cunningham, C.X., Williamson, G.J. & Bowman, D.M.J.S. (2024) Increasing frequency and intensity of the most extreme wildfires on Earth. *Nat. Ecol. Evol.*, 8, 1420–1425.
- DeLuca T.H. & Sala A. (2006). Frequent fire alters nitrogen transformations in ponderosa pine stands of the inland northwest. *Ecology* 87, 2511-2522.
- Farris, C.A., Baisan, C.H., Falk, D.A., Yool, S.R. & Swetnam, T.W. (2013) Spatial and temporal corroboration of a fire-scar-based fire history in a frequently burned ponderosa pine forest. *Ecol. Appl.*, 20, 1598–1614.
- Fréjaville, T. & Curt, T. (2014) Pyroclimatic classification of Mediterranean and mountain landscapes of south-eastern France. In: *Advances in forest fire research,* Chapter 4 Fire Risk Assessment and Climate Change, Ed.: Domingos X.. Coimbra University Press, pp. 1249–1255.
- Fréjaville, T., Curt, T. & Carcaillet, C. (2018). Higher potential fire intensity at the dry range margins of European mountain trees. *J. Biogeogr.*, 45, 2003–2015.

- Fulé, P.Z., Taiqui, L. & Mchich, D. (2025) Interactions of fire and forest structure in a relict mesic forest of north Africa. *Int. J. Wildland Fire*, 34.
- Grime, J.P. (1977) Evidence for the Existence of Three Primary Strategies in Plants and Its Relevance to Ecological and Evolutionary Theory. *Am. Nat.*, 111, 1169–1194.
- Hartigan, J.A. & Wong, M.A. (1979) Algorithm AS 136: A K-Means Clustering Algorithm. *J. Royal Stat. Soc. Series C*, 28, 100–108.
- Häusser, M., Szymczak, S., Knerr, I., Bendix, J., Garel, E., Huneau, F., et al., (2021) The Dry and the Wet Case: Tree Growth Response in Climatologically Contrasting Years on the Island of Corsica. *Forests*, 12, 1175.
- Heinselman, M.L. (1973) Fire in the virgin forests of the Boundary Waters Canoe Area, Minnesota. *Quat. Res.*, 3, 329–382.
- Hodgson, D., McDonald, J.L. & Hosken, D.J. (2015) What do you mean, 'resilient'? *Trends Ecol. Evol.*, 30, 503–506.
- Holling, C.S. (1973) Resilience and Stability of Ecological Systems. *Ann. Rev. Ecol. Evol. Syst.*, 4, 1–23.
- Holmes, R. (1983) Computer-Assisted Quality Control in Tree-Ring Dating and Measurement. *Tree-Ring Bull.*, 43, 69-78.
- Keeley, J.E., Pausas, J.G., Rundel, P.W., Bond, W.J. & Bradstock, R.A. (2011) Fire as an evolutionary pressure shaping plant traits. *Trends Plant Sci.*, 16, 406–411.
- Lebourgeois, F. (2000). Climatic signals in earlywood, latewood and total ring width of Corsican pine from western France. *Ann. For. Sci.*, 57, 155–164.
- Lévesque, M., Rigling, A., Bugmann, H., Weber, P. & Brang, P. (2014) Growth response of five co-occurring conifers to drought across a wide climatic gradient in Central Europe. *Agricul. For. Meteorol.*, 197, 1–12.
- Leys, B., Finsinger, W. & Carcaillet, C. (2014) Historical range of fire frequency is not the Achilles' heel of the Corsican black pine ecosystem. *J. Ecol.* 102, 381-395.
- Lockwood, J.L. & Pimm, S.L. (1994). Biological Diversity: Species: would any of them be missed? *Curr. Biol.*, 4, 455–457.
- Luterbacher, J., Dietrich, D., Xoplaki, E., Grosjean, M. & Wanner, H. (2004) European Seasonal and Annual Temperature Variability, Trends, and Extremes Since 1500. Science. *Science*, 303.
- Malevich, S., Guiterman, C. & Margolis, E. (2018) burnr: Fire History Analysis and Graphics in R. *Dendrochronologia*, 49, 9-15.
- Martín-Benito, D., Gea-Izquierdo, G., del Río, M. & Cañellas, I. (2008) Long-term trends in dominant-height growth of black pine using dynamic models. *For. Ecol. Manag.*, 256, 1230–1238.
- Moritz, M.A., Parisien, M.-A., Batllori, E., Krawchuk, M.A., Van Dorn, J., Ganz, D.J., et al., (2012) Climate change and disruptions to global fire activity. *Ecosphere*, 3, art49.
- Niccoli, F., Esposito, A., Altieri, S. & Battipaglia, G. (2019) Fire Severity Influences Ecophysiological Responses of *Pinus pinaster* Ait. *Front. Plant Sci.*, 10.
- Pauling, A., Luterbacher, J., Casty, C. & Wanner, H. (2006) Five hundred years of gridded high-resolution precipitation reconstructions over Europe and the connection to large-scale circulation. *Clim. Dyn.*, 26, 387–405.

- Pellegrini, A.F., Anderegg, L., Pinto-Ledezma, J.N., Cavender-Bares, J., Hobbie, S.E. & Reich, P.B. (2023) Consistent physiological, ecological and evolutionary effects of fire regime on conservative leaf economics strategies in plant communities. *Ecol. Lett.*, 26, 597–608.
- Pickett, S.T.A. & White, P.S. (1985) *The ecology of natural disturbance and patch dynamics*. Academic Press, Orlando, Florida, pp. 1-42.
- Roshan, A. & Biswas, A. (2023) Fire-induced geochemical changes in soil: Implication for the element cycling. *Sci. Tot. Environ.* 868, 161714.
- Rubino, M., Etheridge, D.M., Thornton, D.P., Howden, R., Allison, C.E., Francey, R.J., *et al.*, (2019) Revised records of atmospheric trace gases  $CO_2$ ,  $CH_4$ ,  $N_2O$ , and  $\delta^{13}C-CO_2$  over the last 2000 years from Law Dome, Antarctica. *Earth Syst. Sci. Data*, 11, 473–492.
- Ruffault, J., Curt, T., Moron, V., Trigo, R.M., Mouillot, F., Koutsias, N., *et al.*, (2020) Increased likelihood of heat-induced large wildfires in the Mediterranean Basin. *Sci. Rep.*, 10, 13790.
- Şahan, E.A., Köse, N., Güner, H.T., Martin-Benito, D., Gea-Izquierdo, G., Conde, M., et al., (2024) Monitoring intra-annual wood Formation of *Pinus nigra* J.F. Arnold (black pine) to understand the fire seasonality in western Anatolia. *Forests* 15, 494.
- Şahan, E.A., Köse, N., Güner, H.T., Trouet, V., Tavşanoğlu, Ç., Akkemik, Ü., et al., (2022) Multi-century spatiotemporal patterns of fire history in black pine forests, Turkey. For. Ecol. Manag., 518, 120296.
- Sayedi, S.S., Abbott, B.W., Vannière, B., Leys, B., Colombaroli, D., Romera, G.G., et al., (2024) Assessing changes in global fire regimes. *Fire Ecol.*, 20, 18.
- Schwarz, J., Skiadaresis, G., Kohler, M., Kunz, J., Schnabel, F., Vitali, V., et al., (2020). Quantifying Growth Responses of Trees to Drought—a Critique of Commonly Used Resilience Indices and Recommendations for Future Studies. *Curr. For. Rep.*, 6, 185–200.
- Seidl, R., Thom, D., Kautz, M., Martin-Benito, D., Peltoniemi, M., Vacchiano, G., et al., (2017) Forest disturbances under climate change. *Nat. Clim. Change.*, 7, 395–402.
- Swetnam, T.W. (1993) Fire History and Climate Change in Giant Sequoia Groves. *Science*, 262, 885–889.
- Seydi, S.T., Abatzoglou, J.T., Jones, M.W., Kolden, C.A., Filippelli, G., Hurteau, M.D., et al., (2025) Increasing global human exposure to wildland fires despite declining burned area. *Science*, 389, 826–829.
- Turco, M., Rosa-Cánovas, J.J., Bedia, J., Jerez, S., Montávez, J.P., Llasat, M.C., et al., (2018) Exacerbated fires in Mediterranean Europe due to anthropogenic warming projected with non-stationary climate-fire models. *Nat. Com.*, 9, 3821.
- Van Loon, A.F. (2015) Hydrological drought explained. Wires Water, 2, 359-392.
- Zackrisson, O. (1977) Influence of Forest Fires on the North Swedish Boreal Forest. *Oikos*, 29, 22–32.
- Zhang. J., Finley, K.A., Johnson, N.G. & Ritchie, M.W. (2019) Lowering stand density enhancDE es resiliency of Ponderosa pine forests to disturbances and climate change. *For. Sci.*, 65, 496–507.

# Supplementary information

# Changes in the fire resilience of Mediterranean trees in response to climate variability over the past 300 Years

Bulle I. Alberto (1,2,3) \*, Justin Badeau (1,2,4), Frédéric Guibal (4), Aurèle Baretje (2,5), Jean-Christophe Domec (3,6), Christopher Carcaillet (1,2)\*

- (1) École Pratique des Hautes Études, Paris Sciences Lettres University (EPHE-PSL), Paris, France
- (2) Université Claude Bernard Lyon 1, LEHNA UMR5023, CNRS, ENTPE, Villeurbanne, France
- (3) Department of forestry, Bordeaux Sciences Agro-INRAE UMR ISPA, Gradignan, France
- (4) Mediterranean Institute of marine and terrestrial Biodiversity and Ecology, IMBE, CNRS (UMR 7263), Aix Marseille Université, France
- (5) École Normale Supérieure de Lyon, Lyon, France
- (6) Nicholas School of the Environment, Duke University, Durham, North Carolina, USA

Authors for correspondence: <u>bulle.alberto@etu.ephe.psl.eu</u>, <u>christopher.carcaillet@ephe.psl.eu</u>

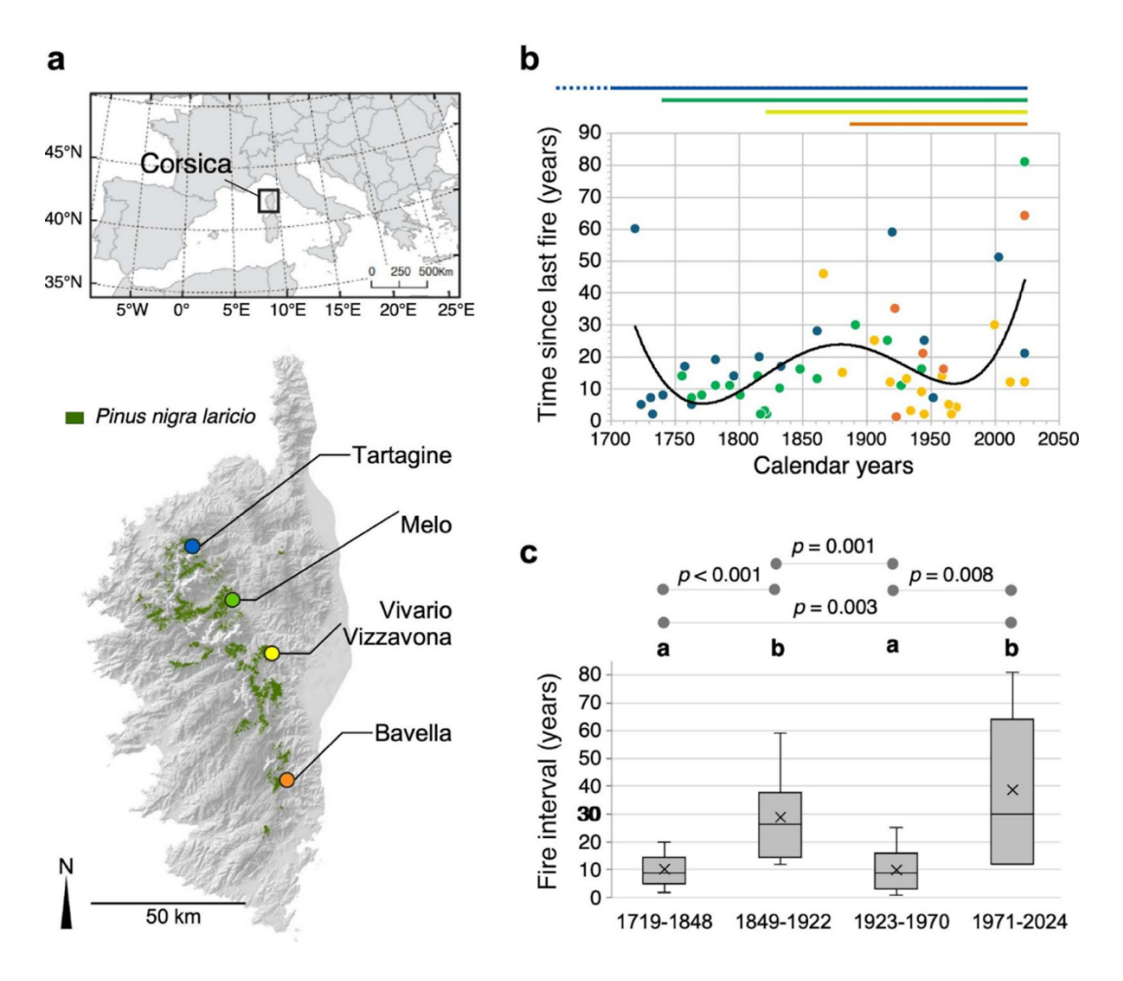


**Figure S1.** (a) Location of the four study sites in Corsica, western Mediterranean Basin, and (**b**,**c**) regime of fire intervals baseline since 1700. In (**b**) the temporal distribution of fire intervals is fitted with a polynomial model to highlight the trend in fire intervals ( $r^2 = 0.32$ ; p < 0.05); the latest value per site corresponds to the time-since-last-fire fixed in 2024; above the graph, horizontal-coloured lines represent length of fire chronology per site with Tartagine (blue) being the longest and Bavella (orange) the shortest. (**c**) Mean fire intervals per period (boxplots); common bold letters indicate means not significantly different by the Wilcoxon-test at p = 0.05); significant differences between MFI are indicated by p-values. More details on fire regime, reconstruction and analysis, in Badeau et al., (2025).

**Table S1.** Description of site characteristics from the northern to southern region of Corsica, France.

Site name	Latitude	Longitude	Elevation (m a.s.l.)				Slope (%)		
Site name	(° north)	(° east)	Min	Max	Mean	Min	Max	Mean	
Tartagine	42.474	8.943	1164	1533	1324	10	90	49	
Melo	42.312	9.072	1193	1617	1439	5	50	29	
Vivario	42.144	9.174	993	1417	1194	15	90	52	
Bavella	41.791	9.238	937	1293	1101	0	80	44	

**Table S2.** Characteristics of samples and their number per plot and site (from north to south), with indication of number and percentage of successful crossdated chronologies per plot.

		Sample type (number)			Crossdated		
Site	Plot	Living	Snag	Log	Stump	no	%
<b>.</b>	01	10			1	9	82
	02	12		1		10	77
	03	11				8	73
Tartagine	04	9	1	3	1	10	71
	05	6		1	3	9	90
	06	4	1			3	60
	01	5		3	7	11	73
	02	5	2	1	8	10	63
Melo	03	4	2	4	6	8	50
	04	9	1	1	3	6	43
	05	8	5	2	6	7	33
	01	6	1		1	7	88
	02	7	1	3	3	9	64
Vivario	03	5	1	1	3	8	80
vivario	04	4			6	8	80
	05	6	3		2	9	82
	06	7	3		1	7	64
Bavella	01	10	1			8	73
	02	10	4			8	57
	03	6		2	3	5	45
	04	10	2			11	92
	05	8	4			9	75
Total	22	162	32	22	54	180	67

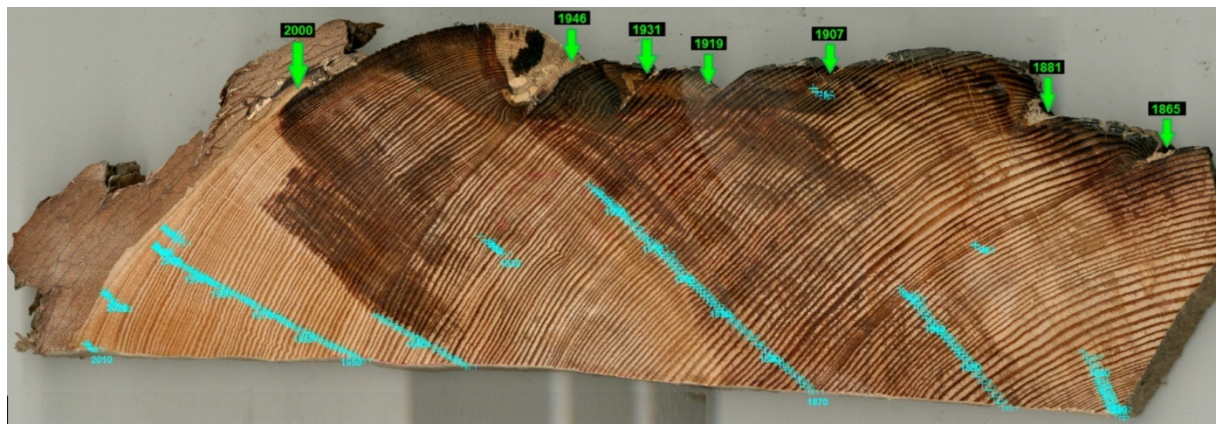


**Figure S2.** Cross section of a black pine, dated from 1824 to 2021 (image: Justin Badeau). Wood sample taken from a living tree (length 25 cm; width 8 cm). Green arrows show seven fire scars 170 years, and blue crosses show rings that have been measured and crossdated.

**Table S3.** Temporal components of fire regime per site considering all fires, from north (left) to south (right); boundary years refer to the first and last recorded fires (from Badeau et al. 2025). The mean fire interval (MFI) characterises the regime, while the coefficient of variation illustrates its stochasticity, which is generally low (< 1.0), and the Min and Max values indicate the range of variability. No significant differences in MFI between sites were found (Wilcoxon test, p = 0.05).

Parameters	Tartagine	Melo	Vivario	Bavella
Fire chronologies				
Length span (years)	345	234	193	73
Boundary years (AD years)	[1659-2003]	[1710-1943]	[1820-2012]	[1887-1960]
Fire number	17	18	15	5
Fire Interval				
Mean ±sd (years) (MFI)	21.5 ±19.1	11.8 ±7.4	13.7 ±12.5	27.4 ±23.8
Coefficient of Variation	0.86	0.58	0.93	0.78
Median (years)	17	11	12	21
Min and Max (years)	2 - 60	2 - 81	2 - 46	1- 64
Wilcoxon tests				
Tartagine	1.00	0.53	0.61	0.77
Melo		1.00	0.95	0.30
Vivario			1.00	0.49
Bavella				1.00

**Table S4.** Statistics of periods of mean fire intervals, their variances (sd, SE), and an indicator of stochasticity (coefficient of variation, CV); a CV-value < 1 means little variation in mean fire interval and lack of stochasticity (Badeau et al., 2025)

Periods	Site number (n)	Intervals (n)	Mean (years)	Standard deviation (years)	Standard error (years)	Coefficient of variation (CV)
1719-1848	2	22	10.0	5.7	1.2	0.57
1849-1922	3	10	28.8	14.9	2.8	0.52
1923-1970	4	15	9.9	7.4	2.4	0.75
1971-2024	4	7	38.7	27.1	4.4	0.70

**Table S5.** Proportions (%) of 16-year fire sequences assigned to each cluster for each MFi period. For some periods, only 2 or 3 clusters were observed, represented by empty cells. Percentages are rounded to the nearest integer. Numbers followed by an asterisk indicate sequences that regain larger TRI after fire than pre-fire reference.

Periods	Cluster 1 (%)	Cluster 2 (%)	Cluster 3 (%)	Cluster 4 (%)
1719-2024	23 *	25	26	27
1719-1848	43	36	21	
1849-1922	46	54 *		
1923-1970	48 *	52		
1971-2024	34	27 *	39	

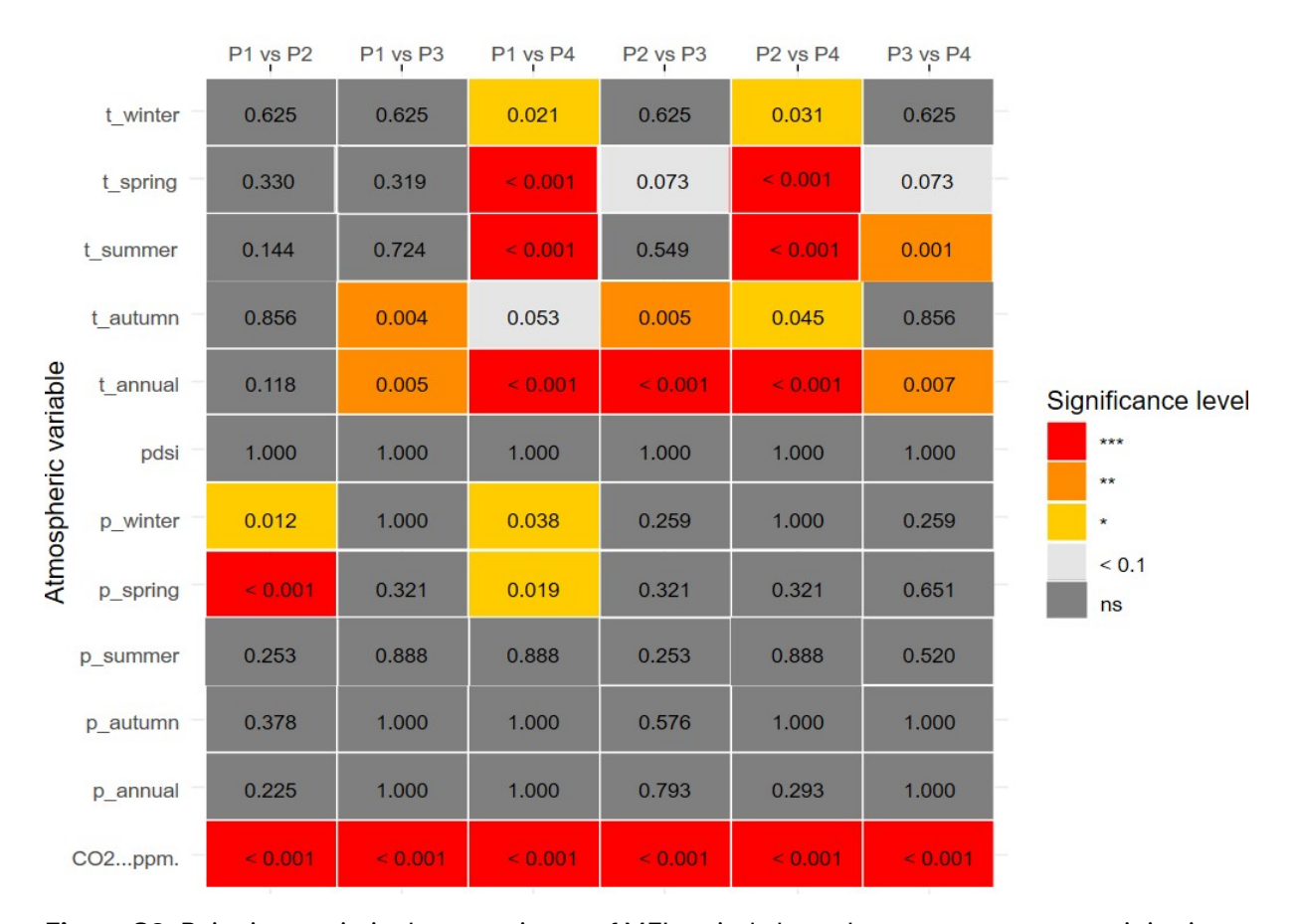


**Figure S3.** Pairwise statistical comparisons of MFI periods based on temperature, precipitation, PDSI (drought index), and atmospheric  $CO_2$  concentration: p-values associated with Wilcoxon tests to determine differences between MFI periods (P1: 1719-1848; P2: 1849-1922; P3: 1923-1970; P4: 1971-2024). \*\*\* = < 0.001, \*\* < 0.01, \* < 0.05 and grey results are non-significative, but 0.1 < p-values < 0.05 are in light grey.